

Mechanical properties and oxidation behaviors of carbon/carbon composites with C-TaC–C multi-interlayer

Zhao-ke Chen · Xiang Xiong · Guo-dong Li ·
Ya-lei Wang

Received: 22 October 2009 / Accepted: 2 March 2010 / Published online: 16 March 2010
© Springer Science+Business Media, LLC 2010

Abstract To improve the mechanical properties and oxidation-resistance properties, a C-TaC–C multi-interlayer structure was introduced in carbon/carbon (C/C) composites by chemical vapor infiltration. Compared with conventional C/C composites, a higher fracture toughness and strength have been achieved by using the C-TaC–C multi-interlayer. In addition, the composites also exhibit a higher preliminary oxidation temperature and a lower mass loss at high temperatures. The oxidation rate of the composites increases with temperature increasing in the range of 700–1300 °C, reaching a maximum value at 1300 °C, then decreases in 1300–1400 °C. A hexagonal structure of Ta₂O₅ phase is obtained when being oxidized at 700–800 °C, and it transforms to an orthorhombic phase at temperatures above 900 °C. The structures of C-TaC–C multi-interlayer are intact without cracks or porosities after being oxidized at 700–800 °C. In 900–1300 °C, the composites are oxidized uniformly with the formation of pores. At temperatures above 1300 °C, there are oxidation and non-oxidation regions with the oxidation process being controlled by diffusion.

Introduction

As aerospace technology develops continuously, there is a rapidly increasing demand for advanced materials for ultra high temperature and aerospace applications, such as rocket

engines and thermal protection systems for space vehicles [1, 2]. Carbon/carbon (C/C) composites are leading candidates for ultra high temperature structural materials due to light weight, low coefficient of thermal expansion (CTE), high strength, high thermal conductivity, dimensional stability, corrosion resistance and shock resistance, ease of machining and low density [3]. However, the use of carbon materials for high temperature application is limited due to their susceptibility to oxidation in air at temperature as low as 400 °C [4]. Efforts have been made to prevent the oxidation of carbon materials by coating C/C with refractory carbides [5, 6] and by doping with boron and phosphorus compounds, which would block the active site for the oxidation of carbon [7, 8]. The former method has a disadvantage of cracks which appear in the protective coating due to the mismatch of CTE between substrate and the coating material, while the doping technique can only provide protection from oxidation with a very limited effect.

Results [9] show that the lateral surfaces of the fibers are attacked first when C/C composites are oxidized in air. Therefore, if refractory carbides can be introduced to the fiber/matrix interphase and form interlayer, the oxidation-resistance of C/C composites will be improved effectively. Labruquère and coworkers [10] coated B–C, Si–B–C, and Si–C phases on carbon fibers as an interlayer in C/C composites to improve the oxidation-resistance properties. Ultramet [11] deposited oxides, nitrides, and carbides on carbon fiber as interface coatings by ultraviolet-activated chemical vapor deposition. Yang et al. [12], Lu et al. [13], and Xiong et al. [14] introduced (BC_x–SiC)_n, C/Si–C–N, and C–SiC–TaC multi-interlayer in C/C composites, respectively. However, the above research had mainly focused on the microstructure observation and mechanical properties. Some studies referred to the development of

Z. Chen · X. Xiong (✉) · G. Li · Y. Wang
State Key Laboratory of Powder Metallurgy, Central South
University, 410083 Changsha, China
e-mail: xiong228@sina.com

Z. Chen
e-mail: pallettechen@163.com

oxidation-resistance properties with a multi-interlayer structure. For example, Pasquier and coworkers [15, 16] had prepared 2D SiC/SiC composites with a multilayered interphase, involving 4 PyC/SiC sequences (PyC-SiC_4); as a result, the lifetime of the composites is significantly improved. Kaur et al. [17] reported the development of oxidation-resistant C–SiC–B₄C composites through the in situ formation of nano-SiC in carbon composites. However, these studies are all about the interlayer in carbon–ceramic composites.

In this work, a C–TaC–C multi-interlayer structure was introduced in C/C composites through fiber coating (interphase) by chemical vapor infiltration (CVI). The mechanical properties and oxidation behaviors at the temperature ranging in 700–1400 °C of C/C composites with C–TaC–C multi-interlayer were studied.

Experimental

Materials preparation

The preparation process of C/C composites with a C–TaC–C multi-interlayer structure is shown in Fig. 1.

Needled and integrated felts with a density of about 0.6 g/cm³ were used as preforms. The carbon fiber was PAN-based (T300, 12 k, Toray, Japan). The needled and integrated felts were prepared by a three-dimensional needling technique, starting with repeatedly overlapping the layers of 0° non-woven fiber cloth, short-cut-fiber web, and 90° non-woven fiber cloth with needle-punching step by step.

PyC interface was firstly deposited by isothermal CVI for 20 h at a temperature in 975–1150 °C and a pressure less than 2 kPa, with C₃H₆ as the reactant gas and Ar the diluent gas. When the density of the preforms was about 0.62 g/cm³, TaC interlayer was deposited by isothermal CVI by using Ar–C₃H₆–TaCl₅ mixtures. The conditions for deposition of TaC were as follows: 800–900 °C, pressure about 600 Pa; and the molar ratio of Ar:C₃H₆:TaCl₅ about 50:3:9. Then the preforms were further deposited with PyC interlayer and densified with resin carbon (by impregnation and carbonization with 2–3 cycles) to obtain C/C composites with C–TaC–C multi-interlayer. The impregnation and carbonization consisted of three steps; Furan resin

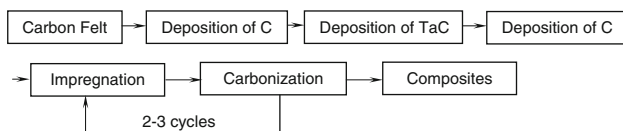


Fig. 1 The preparation process of C/C composites with a C–TaC–C multi-interlayer structure

Table 1 Densities (g/cm³) and relative densities of C/C composites with a C–TaC–C multi-interlayer structure after each step

Step	Felt	After deposition of			Final
		PyC	TaC	PyC	
Density(g/cm ³)		0.56	0.62	1.05	2.02
Relative density (%)		32.6	35.1	38.1	88.5
					2.26

impregnation in preforms, solidification at 180–200 °C for 1 h, and carbonization at 800–1000 °C for 2 h. At last, a bulk C/C composites with a C–TaC–C multi-interlayer structure and sizes of 200 × 100 × 10 mm³ were prepared. The densities and relative densities of the composites after each step are shown in Table 1. The final relative density of the composites is 88.5%, and the calculated TaC volume percent in the composites is about 3%.

Characterization

Seven samples with a size of 40 × 5 × 3 mm³ were cut from the bulk composites and used to test the flexural strength by INSTRON CSS-44100 machine. The gauge size was 30 mm and the crosshead speed was 0.5 mm/min. The load–displacement curves were recorded by computer at the same time. The flexural strength of the composites was estimated according to the following equation [18],

$$\sigma_f = \frac{3PL}{2bh^2}; \quad (1)$$

where σ_f is the flexural strength, MPa; P the maximum load, N; L the gauge size, mm; b and h are the width and thickness of samples, mm.

All oxidation experiments were performed in natural convection air in an Al₂O₃ corundum tube (heated by MoSi₂). The oxidized samples with a size of 10 × 10 × 4 mm³ were cut from the bulk composites, and subjected to a series of thermal cycles in air between oxidation temperature (700–1400 °C) and room temperature (25 °C). The heating rate is about 300 °C/s while the cooling rate is about 200 °C/min. The oxidation time of each thermal cycle is 2, 3, 5, 10, 40 min. In these oxidation experiments, each sample was held at the oxidation temperature for a total of 60 min. After oxidation, the shape of each sample was not destroyed and the composites were not noticeably affected by the thermal cycling. The oxidation rates were determined by calculating the mass loss per square centimeter and per hour of the composites;

$$\alpha = \frac{\Delta m}{A \cdot t}; \quad (2)$$

where α is the oxidation rate in mg/cm² h, Δm the mass change in mg, A the area of the composites in cm², t the oxidation time in h.

The mass change of sample during oxidation process was measured using an AdventurerTM electronic balance with a precision of 0.1 mg. Phase composition of sample before and after oxidation was examined by a D/max 2550VB + 18 kW rotating target XRD spectroscopy. Microstructure was analyzed by a JEOL-6360LV scanning electron microscopy (SEM).

Results and discussion

Microstructures

Figure 2 is the microstructure of the C/C composites. The C/C composites are mainly composed of carbon fibers, multi-interlayer, resin carbon, pores, and cracks. The first layer of the multi-interlayer is C, whereas the following layers are TaC (white phase) and C successively. TaC can be deposited uniformly in the vertical bundles, transverse bundles and short-cut-fiber webs of the composites. The successive pyrocarbon and resin carbon are the main densification constituents of the composites, which mainly fills up the inter-bundle pores in the composites. Resin carbon will shrink in carbonization, which may result in cracks in the composites. Pores result from incomplete densification by the resin impregnation/carbonization steps.

The insert figure shows the structure of the C-TaC-C multi-interlayer. TaC interlayer has a columnar shape, and the combination of C, TaC, and C is compact with no crack in the interface.

By CVI methods, C-TaC-C had been successfully introduced in C/C composites as multi-interlayer (instead of pure pyrocarbon).

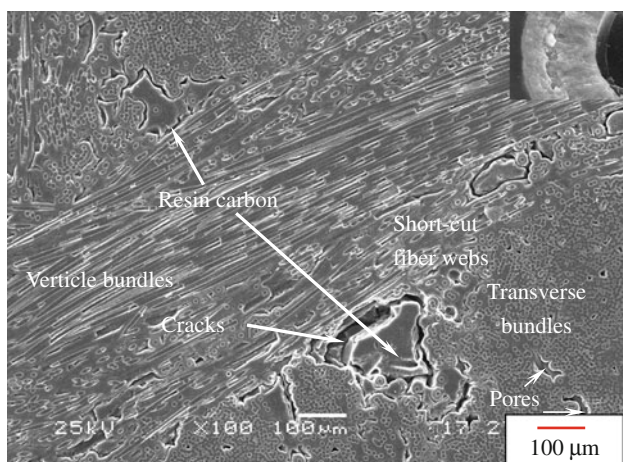


Fig. 2 Microstructures of the composites and C-TaC-C interlayer (the insert figure)

Mechanical properties

The bending strengths of C/C composites with a C-TaC-C multi-interlayer structure are 235–298 MPa, which are superior to the value of 166 MPa of conventional C/C composites. The load–displacement curves of C/C composites with or without C-TaC-C multi-interlayer were shown in Fig. 3.

Conventional C/C composites fail in a brittle manner (curve a); while C/C composites with a C-TaC-C multi-interlayer show ‘elastic–plastic’ manner, as shown in Fig. 4.

There is not any fiber pull-out in the fractograph of conventional C/C composites (Fig. 4a). When C-TaC-C multi-interlayer is introduced, large amounts of fibers, fiber clusters and multi-interlayer are pulled out (Fig. 4b). The C-TaC-C multi-interlayer, which is located between carbon fiber and resin carbon matrix, provides additional fracture mechanisms of multi-interlayer pull-out for the composites. Compared with conventional C/C composites, a higher fracture toughness and strength are achieved.

Oxidation behavior

The retention percentages of weight of the composites as a function of oxidation time at different temperatures are shown in Fig. 5.

At 700 and 800 °C, little mass losses are observed; while the mass losses of conventional C/C composites are obviously above 50%. This suggests that the preliminary oxidation temperature of C/C composites with a C-TaC-C multi-interlayer is improved. Compared with conventional C/C composites, C/C composites with a C-TaC-C multi-interlayer also exhibit a lower mass loss at high temperatures.

The logarithm of oxidation rate ($\ln \alpha$) as a function of reciprocal of temperature is presented in Fig. 6.

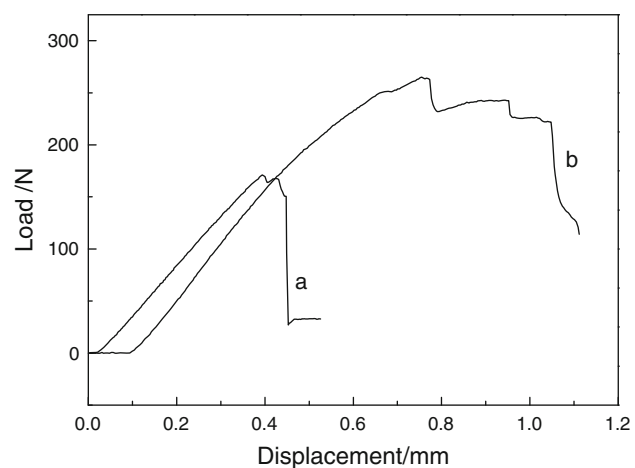


Fig. 3 Load–displacement curves of C/C composites with or without multi-interlayer; (a) C/C; (b) C/C with C-TaC-C multi-interlayer

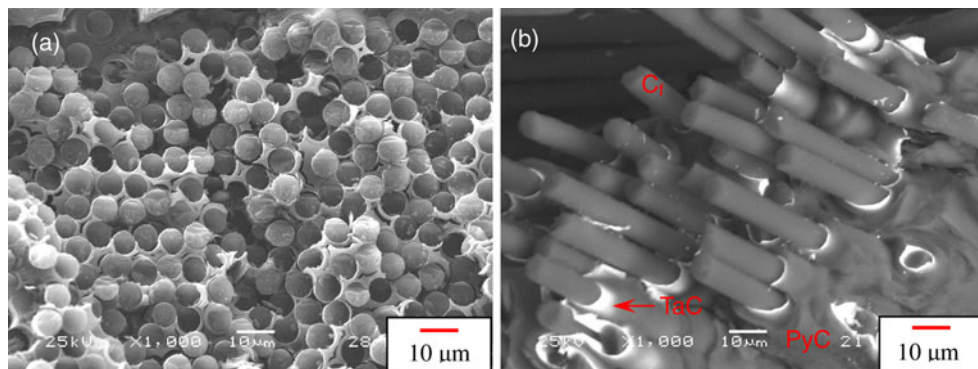


Fig. 4 Fractographs of C/C composites with or without multi-interlayer **(a)** C/C; **(b)** C/C with C-TaC-C multi-interlayer

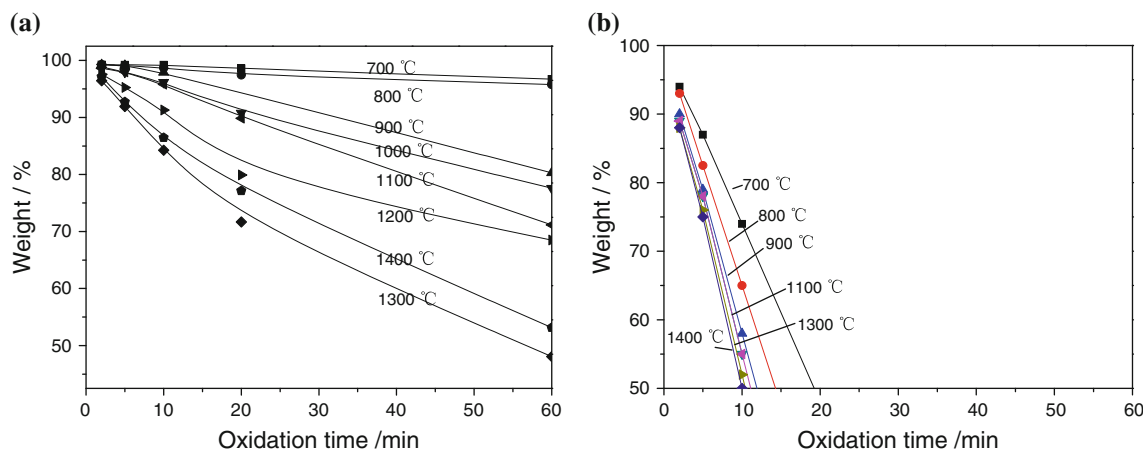


Fig. 5 Retention percentages of weight of the composites as a function of time at different temperatures **(a)** C/C composites with C-TaC-C; **(b)** C/C composites

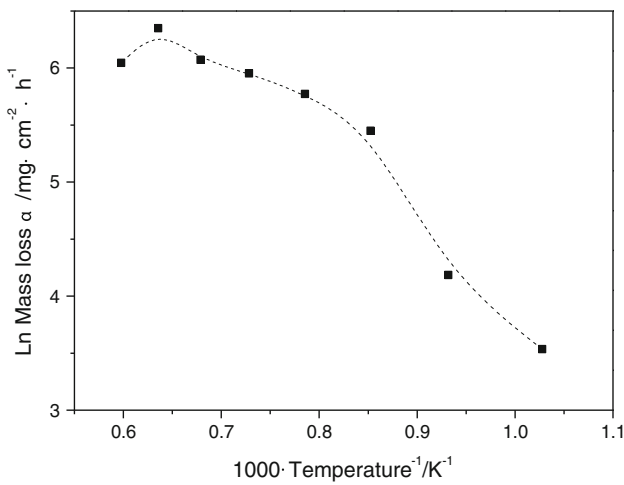


Fig. 6 Logarithm of oxidation rate as a function of reciprocal of temperature

Ln α increases with temperature acutely in 700–900 °C, slowly in 900–1300 °C, and then decreases with temperature in 1300–1400 °C.

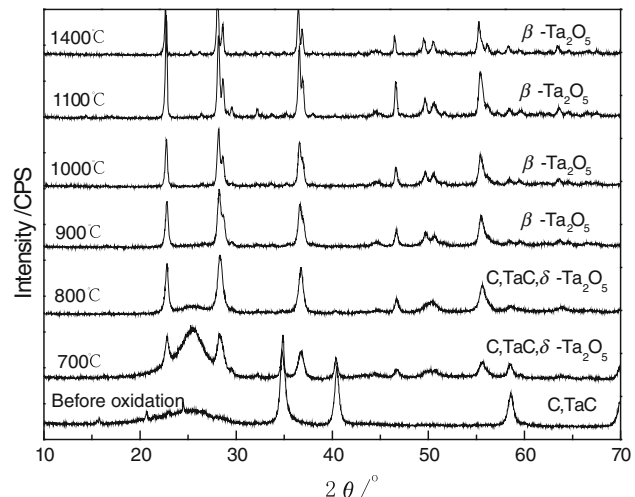


Fig. 7 Phase compositions of the composites before and after being oxidized at different temperatures

Figure 7 presents phase compositions of the composites before and after oxidation for 60 min at different temperatures.

At 700–800 °C, the oxide layer is very thin and X-ray diffraction patterns from C, TaC phases in the composites are observed. In addition, the residual oxide product is only Ta_2O_5 phase but with different crystal structures. At 700–800 °C, a Ta_2O_5 phase with hexagonal structure ($\delta\text{-Ta}_2\text{O}_5$) is obtained, which then transforms to an orthorhombic structure (L- Ta_2O_5 or $\beta\text{-Ta}_2\text{O}_5$) when oxidation temperature increases to 900 °C. These results are in agreement with the reported values in literature [19].

Microstructures of the composites after oxidation for 60 min at different temperatures are shown in Fig. 8.

At 700–800 °C, only a few surface of the composites had been oxidized (Fig. 8a). In the composites, C fiber and C-TaC-C multi-interlayer are intact without cracks or porosities (Fig. 8b). At 900–1300 °C, the composites are oxidized uniformly (Fig. 8c). In the composites, pores are formed at the place of carbon phases (carbon fibers and

carbon matrix), indicating that C phase is rapidly oxidized (Fig. 8d). This gives an easy access of oxygen to the center of the composites. At 1400 °C, the composites consist of two distinct structural scales, namely, oxidation region and non-oxidation region (Fig. 8e). In oxidation region, TaC interlayer is oxidized seriously and forms a porous Ta_2O_5 phase (Fig. 8f). In non-oxidation region, C fiber and C-TaC-C multi-interlayer in the composites keep intact and not being oxidized.

Oxidation mechanism

From Fig. 7, it shows that TaC interlayer is oxidized at 700 °C and form $\delta\text{-Ta}_2\text{O}_5$ phase. The oxidation of TaC to $\delta\text{-Ta}_2\text{O}_5$ phase is a mass gain process, which can offset the mass loss of the oxidation of C. This may be the main reason for the little mass loss of composites at 700–800 °C.

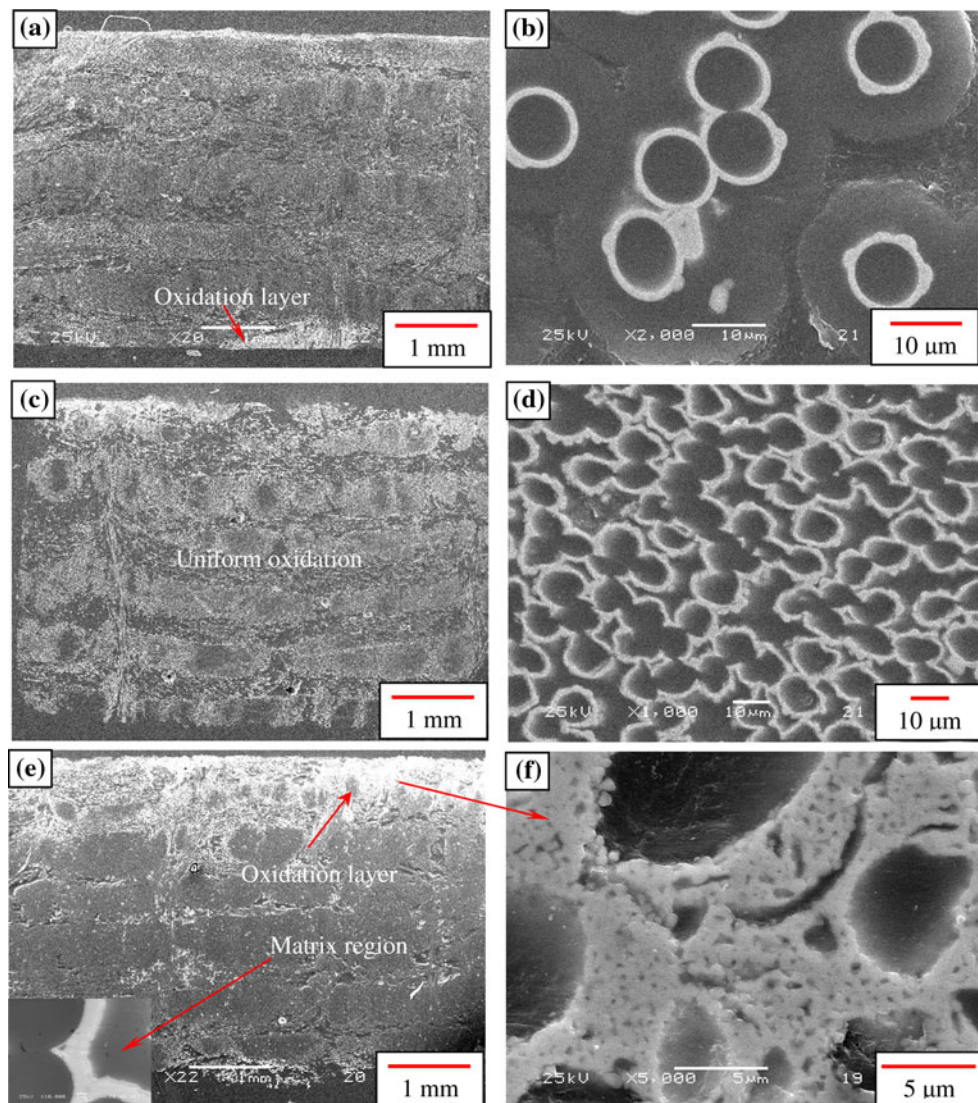


Fig. 8 Microstructures of the composites after oxidation for 60 min at (a, b) 700–800 °C, (c, d) 900–1300 °C, (e, f) 1400 °C

The perfect microstructure in Fig. 8a, b also indicates the oxidation of the composites is very slight.

At 900–1300 °C, TaC interlayer is oxidized to form β -Ta₂O₅ phase. In fact, TaO₂ is also formed in this temperature region. In the oxidation process, TaO₂ is vapor and can diffuse in the composites; a small part of TaO₂ can react with O₂ in the composites at the place with a higher oxygen partial pressure and form Ta₂O₅; while most TaO₂ will escape from the composites. Therefore, the pores and cracks in the composites can not be filled by the oxidation of TaC. This makes a rapid channel of oxygen to the center of the composites. In this case, carbon phases oxidize extensively and burns away. As can be seen from Fig. 8d, lots of pores are formed at the place of C phases in the composites. Further, these pores provide a rapid diffusion route to the escape of TaO₂, CO and the infiltration of oxide gas in the composites, resulting in the deterioration oxidation of the composites. Therefore, the composites show an obvious mass loss (see Fig. 6) after being oxidized at 900–1300 °C. The evaporation of TaO₂ and the rapid oxidation of C phases are the main reasons for the acute mass loss of the composites at 900–1300 °C.

At 1400 °C, TaC turns to Ta₂O₅ only. TaC can be oxidized with a 103% volume gain to prevent oxygen access to the interfacial zones. C phases can be protected perfectly by the oxidation of TaC in the composites. In this case, the weight gain from oxidation of TaC to Ta₂O₅ is higher than the weight loss of oxidation of C. Therefore, the oxidation rate of the composites decreases and there is a change in the slope of the oxidation curve in Fig. 6. From the results of oxidation rate with a function of temperature and microstructure analyses, it can be concluded that the oxidation process was controlled by diffusion at temperatures up to 1300 °C.

Conclusions

By studying the mechanical properties and oxidation behaviors of C/C composites with C-TaC–C multi-interlayer, we can make the following conclusions:

Compared with conventional C/C composites, a higher fracture toughness and strength are achieved for C/C composites with a C-TaC–C multi-interlayer structure. In addition, the composites also exhibit a higher preliminary oxidation temperature and a lower mass loss at high temperatures.

The oxidation rate ($\ln \alpha$) of the composites increases with temperature within 700–1300 °C, reaching a maximum value at 1300 °C, then decreases within 1300–1400 °C.

At 700–800 °C, a Ta₂O₅ phase with a hexagonal structure is obtained and transforms to an orthorhombic structure when the oxidation temperature is above 900 °C. The structures of C-TaC–C multi-interlayer are intact without cracks or holes after being oxidized at 700–800 °C; At 900–1300 °C, the composites are oxidized uniformly with pores formed at the place of carbon phases; At temperature above 1300 °C, the composites consist of oxidation and non-oxidation regions with the oxidation process being controlled by diffusion.

In order to improve the oxidation resistance of C/C composites with C-TaC–C multi-interlayer further, an outer coating should be prepared on this kind of composites, which deserve further study.

Acknowledgements This research work is supported by National Natural Science Foundation of China under the Grant No. 50872154 and by Creative research group of National Natural Science Foundation of China under the Grant No. 50721003.

References

1. Tang SF, Deng JY, Wang SJ, Liu WC, Yang K (2007) Mater Sci Eng A 465:1
2. Raman V, Bhatia G, Mishra A, Sengupta PR, Saha M, Rashmi (2005) Mater Sci Eng A 412:31
3. Virgil'ev YS, Kalyagina IP (2004) Inorg Mater 40:S33
4. Guo WM, Xiao HN (2007) Carbon 45:1058
5. Wunder V, Popovska N, Wegner A, Emig G, Arnold A (1998) Surf Coat Technol 100–101:329
6. Zhu YC, Ohtani S, Sato Y, Iwamoto N (2000) Carbon 38:501
7. Manocha LM, Manocha S, Patel KB, Glogar P (2000) Carbon 38:1481
8. Cairo CAA, Florian M, Graca MLA, Bressiani JC (2003) Mater Sci Eng A 358:298
9. Han JC, He XD, Du SY (1995) Carbon 33:473
10. Labruquère S, Blanchard H, Pailler R, Naslain R (2002) J Eur Ceram Soc 22:1011
11. Fiber interface coatings (2009-10-22) US Ultramet. http://www.ultramet.com/fiber_interface_coatings.html. Accessed 2009
12. Yang WB, Zhang LT, Liu YS, Cheng LF, Zhang WH (2007) Appl Compos Mater 14:277
13. Lu GF, Qiao SR, Zhang CY, Hou JT, Jia DC, Zhang YB (2008) Compos Part A 39:1467
14. Xiong X, Wang YL, Chen ZK, Li GD (2009) Solid State Sci 11:1386
15. Pasquier S, Lamon J, Naslain R (1998) Compos Part A 29A:1157
16. Bertrand S, Droillard C, Pailler R, Bourrat X, Naslain R (2000) J Eur Ceram Soc 20:1
17. Kaur M, Kumar S, Sengupta PR (2009) J Mater Sci 44:2128. doi: [10.1007/s10853-009-3307-0](https://doi.org/10.1007/s10853-009-3307-0)
18. Xu YD, Cheng LF, Zhang LT, Yin HF, Yin XW (2001) Mater Sci Eng A 300:196
19. Krishnan RR, Gopchandran KG, MahadevanPillai VP, Ganesan V, Sathe V (2009) Appl Surf Sci 255:7126